
SCALING FEDERATED LEARNING SOLUTIONS WITH KUBERNETES FOR SYNTHESIZING HISTOPATHOLOGY IMAGES

Andrei-Alexandru Preda¹, Iulian-Marius Tăiatu¹, Dumitru-Clementin Cercel^{1*}

¹National University of Science and Technology POLITEHNICA Bucharest, Bucharest, Romania

ABSTRACT

In the field of deep learning, large architectures often obtain the best performance for many tasks, but also require massive datasets. In the histological domain, tissue images are expensive to obtain and constitute sensitive medical information, raising concerns about data scarcity and privacy. Vision Transformers are state-of-the-art computer vision models that have proven helpful in many tasks, including image classification. In this work, we combine vision Transformers with generative adversarial networks to generate histopathological images related to colorectal cancer and test their quality by augmenting a training dataset, leading to improved classification accuracy. Then, we replicate this performance using the federated learning technique and a realistic Kubernetes setup with multiple nodes, simulating a scenario where the training dataset is split among several hospitals unable to share their information directly due to privacy concerns.

1 Introduction

Lack of sufficient training data has always been a problem in training machine learning models [Bansal et al., 2022]. This problem has become more pronounced over time, as state-of-the-art models have become larger and more data-hungry, such as the Transformer [Vaswani et al., 2017] family. Augmenting datasets means generating new training samples from existing ones using various techniques. Generative Adversarial Networks (GANs) [Goodfellow et al., 2014] are suitable for generating synthetic samples, especially synthetic images. These networks involve training two neural networks that compete against each other and have produced good results in the past [Odena et al., 2017, Jose et al., 2021].

In recent years, the public has become more aware of the importance of data privacy, especially in the medical and telecommunications fields. Federated learning [McMahan et al., 2017] is a technique that allows training models in a non-centralized manner by distributing a model to independent clients, which then train it locally using their private data. In this way, training data do not have to leave the environment where they are safely stored and are prone to being shared. This technique is especially relevant in the medical domain, which deals with sensitive data [Feki et al., 2021, Pfitzner et al., 2021].

In this work, we experiment with several GAN variants (i.e., conditional GAN [Mirza and Osindero, 2014], Wasserstein GAN with gradient penalty [Gulrajani et al., 2017], and auxiliary classifier GAN [Odena et al., 2017]) to produce histopathological images and build a system capable of augmenting training datasets. Since the medical domain involves working with sensitive information, we then try to address realistic privacy concerns by incorporating federated learning into the process, simulating a situation where multiple hospitals would train this machine learning model without risking exposing their patients' data. Finally, we use Kubernetes (<https://kubernetes.io>, accessed on 10 March 2025) to test the project in a production-ready environment. The performance of the resulting system is evaluated by analyzing the images it produces. In addition, we assess their usefulness by demonstrating their effectiveness in a downstream task: training a separate classifier for medical images and checking to improve its classification capabilities when adding our synthetic data.

Our main contributions are as follows:

1. Comparing several GAN architectures for synthesizing histopathology images of colorectal cancer;

*Corresponding author: dumitru.cercel@upb.ro.

2. To the best of our knowledge, this is the first time the federated setting has been used to train GANs on the TCGA-CRC-DX dataset [Kather, 2020] we use;
3. Experimenting to replicate centralized performance in a production-ready federated setting;
4. Analyzing data produced by GANs to check for common errors and suggest improvements;
5. Publishing our experimental code (<https://github.com/pandrei7/paper-synthesizing-histopathology>, accessed on 10 March 2025) for the wider public to ease reproducibility.

2 Related Work

2.1 Generative Adversarial Networks

GANs [Goodfellow et al., 2014] refer to a framework for training neural networks capable of producing fake content with a distribution similar to that of real content. The framework uses an adversarial process to train two separate networks: a *generator* and a *discriminator*. The objective of the generator is to produce realistic samples when given noise from a fixed distribution as input, while the discriminator tries to discern between real and fake samples. The two networks compete throughout the training process until the discriminator can no longer distinguish between real and fake input.

Since their introduction, multiple variants of GAN have appeared. One of these variants is the auxiliary classifier GAN (ACGAN) [Odena et al., 2017]. Unlike the original GAN, the generator of the ACGAN is conditioned on class labels, which later allows the generation of data of multiple specified types. Similarly, the discriminator is tasked with detecting whether a sample is real or fake and predicting the sample’s class label.

It should be noted that while GANs have been used in the past [Mino and Spanakis, 2018, Esser et al., 2021, Fang et al., 2022, Năstăsescu and Cercel, 2022] with good results, they tend to be challenging to train, manifesting problems such as overfitting and mode collapse, which refers to the generation of a limited number of types of samples that are exploited by a discriminator weakness [Xu et al., 2024].

2.2 Vision Transformers

The Transformer architecture [Vaswani et al., 2017] was introduced in 2017, initially for the task of machine translation, but has since found many other uses, especially in the domain of natural language processing [Paraschiv and Cercel, 2019, Vlad et al., 2019, Tanase et al., 2020, Vlad et al., 2020a,b, Paraschiv et al., 2020, Echim et al., 2023]. Some of its characteristics include the encoder-decoder architecture and an attention mechanism. The vision Transformer (ViT) [Dosovitskiy et al., 2020] brings these ideas to the computer vision domain, splitting images into patches, linearly embedding them, adding position embeddings, and feeding them to a standard Transformer. For example, ViT has been used in medical applications as a component of the MedViT models [Manzari et al., 2023].

2.3 Federated Learning

Federated learning [McMahan et al., 2017] is a machine learning technique that allows training models to use datasets distributed on multiple *clients* to avoid sharing private information with a centralized *server*. At a high level, this technique works by having each client train a model on their private dataset and sending these models or only their gradients to the server, where they are aggregated. In this way, the training data never have to leave the clients. The server is in charge of coordinating the process until the training is over.

Federated learning is essential in the medical domain, where hospitals or research centers tend to have sensitive data that should not be shared, for example, for ethical reasons.

2.4 Histopathology Image Analysis and Generation

Histopathology is the study of tissue disease. An application of machine learning related to histopathology is the diagnosis of diseases by studying images of tissues and cells, which can be formulated as a classification problem. Histopathological images are more diverse, complex, and intricate than natural images, making this task difficult [Fang et al., 2022]. In addition, the datasets for this task tend to be smaller and imbalanced, making generating synthetic images quite important. Our work is inspired by previous research that attempted to solve this problem. For example, [Xu et al., 2024] uses a diffusion model Ho et al. [2020] enhanced with a Transformer to generate histopathological

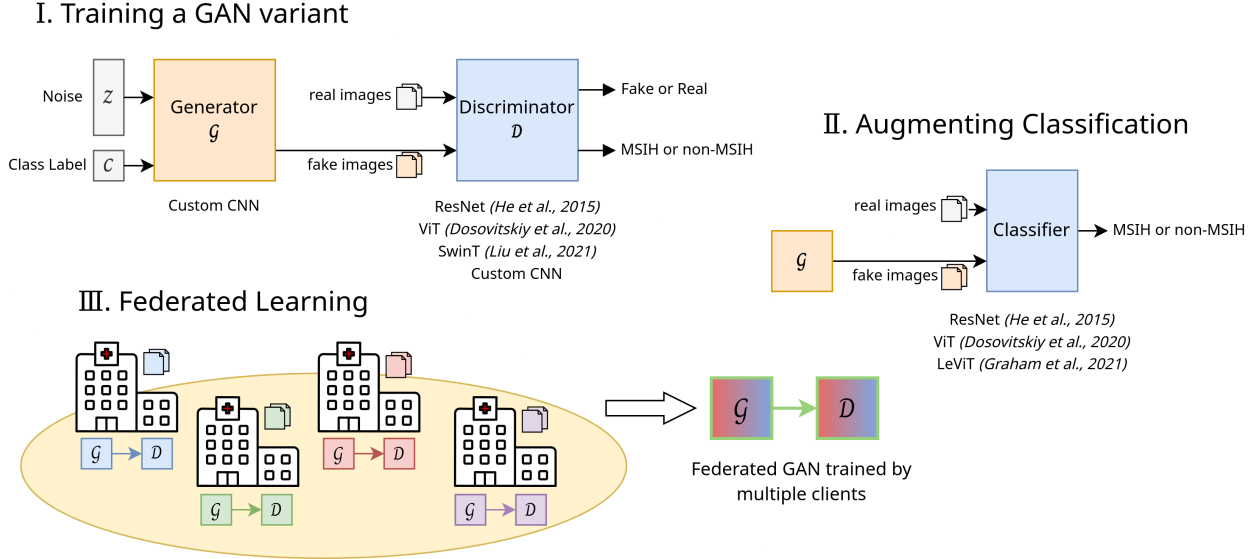


Figure 1: Summary of the proposed approach: testing different types of GANs for histopathology images, using synthetic images to improve classification, and exploring this method in a federated setting for increased data privacy.

images. In contrast, [Zedda et al., 2023] incorporates a hierarchical ViT [Dosovitskiy et al., 2020] into a custom architecture called a Hierarchical Pretrained Backbone Vision Transformer to classify histopathological images.

3 Method

3.1 Data Augmentation

3.1.1 GAN-based Augmentations

As shown in Figure 1, our solutions for generating synthetic images are based on different variants of the discriminator network. Specifically, we started by experimenting with a convolutional neural network (CNN) O’Shea and Nash [2015], namely ResNet [He et al., 2016], and then moved to Transformer architectures, such as the original ViT [Dosovitskiy et al., 2020] and the Swin Transformer (SwinT) [Liu et al., 2021], which obtained better results.

In all experiments, the generator is a *Custom CNN*, consisting of a convolutional neural network with three layers, the LeakyReLU activation function, and operations such as batch normalization, upsampling, and dropout. To control the labels of synthetic images, we condition the generator on the class embeddings learned throughout the training. These embeddings can be added as an additional dimension to the noise tensor. However, we obtained better results by multiplying each input channel with the embedding instead; our embeddings were shaped like image channels.

There are multiple ways of training GANs. We experimented with the regular conditional GAN (CGAN) [Mirza and Osindero, 2014], the Wasserstein GAN [Arjovsky et al., 2017] variant that adds a gradient penalty to stabilize training (WGAN-GP) [Gulrajani et al., 2017], and with the auxiliary classifier GAN (ACGAN) [Odena et al., 2017], which requires the discriminator to guess both the image label and its origin.

3.1.2 Geometric Transformations

To train better classifiers, we use data augmentation through geometric transformations: crops, horizontal flips, and affine transformations up to at most 45 degrees. In addition, as a data preprocessing step, all pixel values are normalized. These geometric transformations are also applied to the synthetic images generated with GANs.

3.2 Classification Models

One way we tried to evaluate the quality of the synthetic images produced by GANs was to check their usefulness for classification through augmentation. We handle classification starting from pre-trained models and changing

their classification heads before fine-tuning them on our dataset. We used multiple classifiers with different internal mechanisms:

- ResNet [He et al., 2016]: ResNet is a popular neural network architecture for computer vision and is one of the first to demonstrate the effectiveness of residual connections in training deeper models. This architecture processes images using convolutions, residual blocks, and downsampling operations. We specifically used the *ResNet 50* variant [maintainers and contributors, 2016] in our experiments, which contains five different stages, each containing several convolutional and batch normalization layers, as well as the ReLU activation function. This classifier was initialized with weights pre-trained on the ImageNet dataset [Deng et al., 2009].
- ViT [Dosovitskiy et al., 2020]: The ViT architecture incorporates the attention mechanism into a solution for computer vision by splitting images into several parts and applying attention to their embeddings. These models use several Transformer encoder layers, involving both attention operations and fully connected layers, and using the GELU activation function. We specifically used the *ViT B 16* and *ViT L 16* variants present in TorchVision [maintainers and contributors, 2016], with 86 million trainable parameters and 305 million, respectively. These classifiers were also pre-trained on ImageNet before our fine-tuning.
- LeViT [Graham et al., 2021]: The LeViT architecture is a hybrid neural network that combines convolutions and attention. The input is first processed by a series of convolutional layers, then by three stages of modified Transformer blocks. We specifically used the implementation available in the timm library [Wightman, 2019], where the model is called *LeViT Conv 384*. This model had approximately 37 million trainable parameters, and, different from the previous two classifiers, it uses the Hardswish activation function.

3.3 Federated Learning

After obtaining the results in a centralized setting, we try to replicate that performance using federated learning to simulate multiple hospitals that collaborate to train a good model while keeping their data private. Concretely, we perform numerous rounds of training, which involve sampling a few clients, sending them the current aggregate model checkpoint, improving that model for a few epochs separately on each client, and then merging the updated weights to obtain the next aggregate model. We perform weighted averaging using the FedAvg algorithm [McMahan et al., 2017]. The Algorithm 1 shows the pseudocode.

Algorithm 1 Pseudocode for the federated learning algorithm using FedAvg [McMahan et al., 2017]

R = number of rounds to train
 E = number of epochs to train a client during one round
 α = fraction of clients to train in one round
 δ_i = dataset belonging to client i
 $w_{c,i}$ = weight coefficient computed by FedAvg

```

1: procedure TRAINING
2:   model0 ← random GAN initialization
3:   for  $i = 1 \rightarrow R$  do
4:     clients ← sample  $\alpha$  client IDs
5:     for all  $c \in$  clients do
6:       weights $c$  ← ROUND(model $i-1$ ,  $\delta_c$ )
7:     model $i$  ←  $\sum_{c \in \text{clients}} w_{c,i} * \text{weights}_c$ 
8:   return model $R$ 

9: procedure ROUND(model0, dataset)
10:  for  $i = 1 \rightarrow E$  do
11:    model $i$  ← BACKPROPAGATION(model $i-1$ , dataset)
12:  return model $E$ 
  
```

In practice, different clients often have different data distributions, which can affect the training process Feki et al. [2021]. To simulate this scenario, we introduce a class imbalance in every client by assigning more samples from one of the two classes. We call this scenario *the not independent and identically distributed (non-IID)* Feki et al. [2021] and study the effect of the class imbalance rate.

Table 1: Baseline performance on the test set. Augmentation refers to geometric transformations such as crops, flips, and affine transformations.

Model	Augmentation	Accuracy	F1-score
ResNet 50 [He et al., 2016, maintainers and contributors, 2016]	No	.7965	.8800
ResNet 50 [He et al., 2016, maintainers and contributors, 2016]	Yes	.7778	.8663
ViT B 16 [Dosovitskiy et al., 2020, maintainers and contributors, 2016]	Yes	.7952	.8802
ViT L 16 [Dosovitskiy et al., 2020, maintainers and contributors, 2016]	Yes	.8005	.8833
LeViT Conv 384 [Graham et al., 2021, Wightman, 2019]	Yes	.7846	.8713

3.4 Experimental Setup

3.4.1 Dataset

We experimented with the TCGA-CRC-DX dataset [Kather, 2020], which consists of histopathological images 51,918 of colorectal cancer. These belong to patients divided into two categories based on the microsatellite instability (MSI) status: samples from patients with MSI-high form class *MSIH*, and those from patients with MSI-low or with microsatellite stability (MSS) form the *non-MSIH* class. Thus, the dataset is suitable for a binary classification task.

The original images had a resolution of 512×512 , but we resized them to 224×224 to lower the computing resources required. We used the train-test split published on Zenodo (<https://zenodo.org/records/3832231>, accessed on 10 March 2025), which includes 19,557 images in the training set and 32,361 images in the test set, a ratio of 1 : 2.

3.4.2 Hyperparameters

Each variant of GAN was trained for 20–40 epochs, with a learning rate of 10^{-4} (or $3 * 10^{-5}$ for ACGAN with a SwinT discriminator). In general, training the GANs well was fairly difficult and required setting the right hyperparameters. WGAN-GP especially proved to be sensitive to hyperparameters such as n_{critic} (which controls the number of epochs used to train the discriminator) and λ_{GP} (the coefficient for gradient penalty). Setting improper values for these parameters resulted in completely noisy images and an ineffective training process. We used $n_{critic} = 10$ and $\lambda_{GP} = 3$. To search for GAN hyperparameters, we typically started several training runs with various reasonable combinations and stopped them after a small number of epochs. Then, based on the stability of the loss curves and manual inspection of the images produced so far, we trained much longer with the most promising configurations. Although this simple method can be improved, in practice, it helped us find good hyperparameters quickly.

For classification, models were trained for 30–50 epochs with early stopping and a learning rate of 10^{-4} . The images were normalized with the mean and standard deviation suitable for ResNet. The best models were initialized from weights pre-trained on ImageNet.

For federated learning experiments, we trained with a number of 4 or 10 clients for between 10–16 rounds, each round involving the choice of 4 random clients and training them for 4 local epochs; thus, the fraction of clients α mentioned in Algorithm 1 was 40% or 100%, depending on the run.

Experiments were carried out using Python libraries related to PyTorch [Paszke et al., 2019] as follows: Torchvision [maintainers and contributors, 2016], PyTorch Lightning [Falcon and The PyTorch Lightning team, 2019], and Torchmetrics Nicki Skafted Detlefsen et al. [2022]. Federated learning experiments used the Flower framework [Beutel et al., 2022] for Python.

3.4.3 Baselines

To prepare for future experiments, we first set a baseline classification performance for some models on the original dataset. Specifically, we tested four different models: ResNet 50, ViT B 16, ViT L 16, and LeViT Conv 384. The results can be seen in Table 1. ViT L 16 obtained the best F1-score on this dataset, close to 88%.

4 Results

4.1 GAN Comparison

FID scores [Heusel et al., 2017] obtained with different GANs and discriminators can be seen in Table 2. We observed stark differences when training with a CNN-based discriminator instead of a Transformer-based discriminator, with

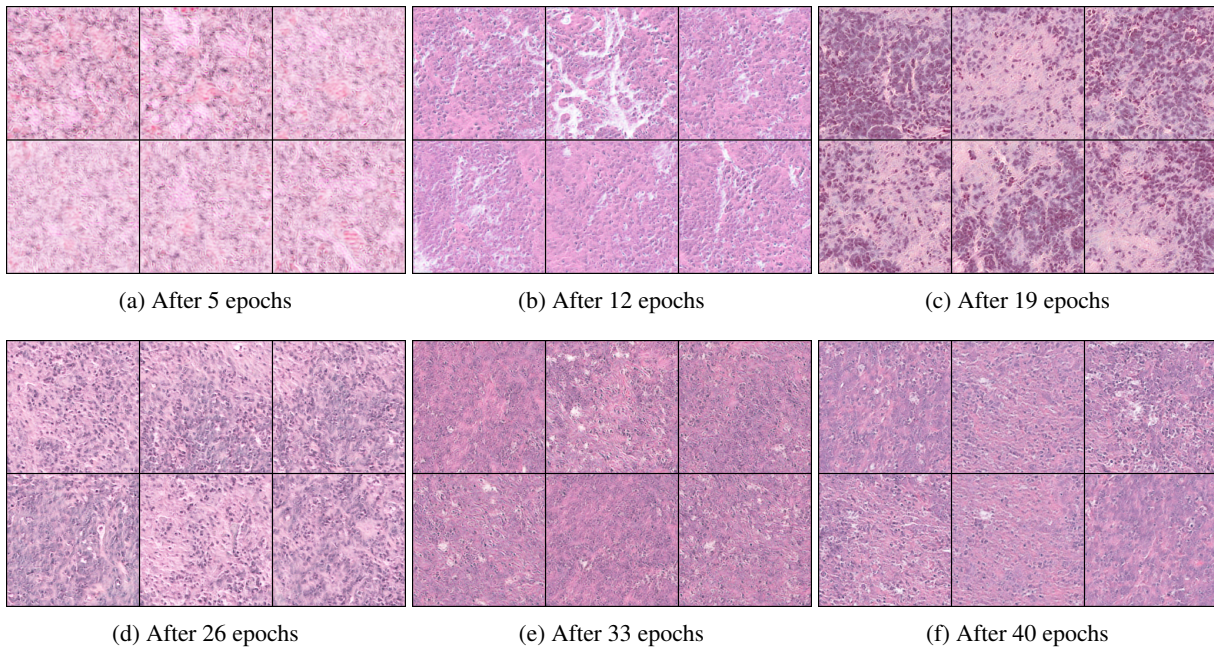


Figure 2: Images generated by ACGAN with a ViT B 16 discriminator.

Table 2: FID scores for different GANs and discriminators (lower is better)².

GAN Type	Discriminator	No. of Epochs	FID (\downarrow)
ACGAN	Custom CNN	30	355.30
	ResNet 18	40	261.86
	ResNet 50	40	143.91
	ViT B 16	28	201.22
		32	223.86
		36	177.00
		40	192.29
	SwinT	40	285.71
CGAN	Custom CNN	30	333.97
	ViT B 16	30	325.36
WGAN-GP	Custom CNN	30	281.47

Transformer discriminators giving better results. More powerful discriminators were able to learn relevant features about the inputs, which in turn helped the generator. The attention mechanism employed by ViT, combined with the pre-trained initialization weights that identify visual features fit for image classification, gave it an edge in processing histopathological images, which are very intricate. Similarly, having different architectures for the generator and discriminator meant that we encountered fewer situations where one component of the GAN exploited a weakness of the other, leading the system to diverge, as happened more often when using only CNNs.

Furthermore, architectures such as the CGAN had a harder time producing images with any amount of detail, with their output usually being noisy color gradients. The extra classification task imposed by ACGAN allowed the discriminator to develop better features, allowing the generator to produce images with more detail. Figure 2 displays the images produced by ACGAN during a training run using a ViT B 16 discriminator. As seen through visual inspection in Figure 2, these results also reinforce the idea that image quality fluctuates during training. However, it should be noted that images with the lowest FID did not always look reasonable on visual inspection and cannot be judged based solely on this metric.

²For the ViT B 16 model, we evaluate image quality at multiple points during training to get a sense of how it changes in time (all these scores come from a single, continuous training run).

Table 3: Results for different classifiers with synthetic data from ACGAN. All synthetic images were generated by a CNN trained using an ACGAN, but with different discriminators. Improvements over the baseline (no synthetic data) are highlighted in bold.

ACGAN Discriminator	Data Type	ResNet 50		ViT B 16		ViT L 16		LeViT Conv 384	
		Acc.	F1	Acc.	F1	Acc.	F1	Acc.	F1
-	only real	.7965	.8800	.7952	.8802	.8005	.8833	.7846	.8713
ResNet 18 @40 epochs	only generated	.8052	.8910	.6717	.7979	.6684	.7890	.8102	.8949
	generated + real	.7866	.8718	.7870	.8720	.7985	.8816	.8078	.8891
ResNet 50 @40 epochs	only generated	.7462	.8437	.7410	.8431	.7456	.8451	.5727	.6897
	generated + real	.7777	.8660	.7907	.8731	.7901	.8736	.7806	.8698
ViT B 16 @28 epochs	only generated	.8167	.8979	.4694	.5853	.5030	.6243	.7679	.8664
	generated + real	.7763	.8651	.7907	.8745	.7926	.8774	.7641	.8580
ViT B 16 @32 epochs	only generated	.4318	.5382	.3356	.3954	.3884	.4789	.3545	.4056
	generated + real	.7903	.8755	.7847	.8711	.7893	.8765	.7814	.8668
ViT B 16 @36 epochs	only generated	.4432	.5521	.5002	.6237	.5152	.6417	.3901	.4724
	generated + real	.7842	.8718	.7908	.8768	.7755	.8638	.7916	.8763
ViT B 16 @40 epochs	only generated	.4333	.5301	.7605	.8594	.5215	.6479	.6296	.7549
	generated + real	.7730	.8619	.7798	.8667	.7852	.8731	.7957	.8800
SwinT @40 epochs	only generated	.8055	.8910	.8257	.9043	.7748	.8722	.8225	.9025
	generated + real	.8063	.8869	.7842	.8704	.7958	.8808	.7840	.8716

Table 4: Results for different classifiers with synthetic data from various GANs. All synthetic images were generated by a CNN trained using GANs other than ACGAN. Improvements over the baseline (no synthetic data) are highlighted in bold.

GAN Type	GAN Discriminator	Data Type	ResNet 50		ViT B 16		ViT L 16		LeViT Conv 384	
			Acc.	F1	Acc.	F1	Acc.	F1	Acc.	F1
-	-	only real	.7965	.8800	.7952	.8802	.8005	.8833	.7846	.8713
CGAN	Custom CNN	only generated	.7379	.8465	.7483	.8520	.5463	.6787	.5720	.7117
		generated + real	.7939	.8780	.7695	.8616	.7789	.8689	.7874	.8737
CGAN	ViT B 16	only generated	.8363	.9108	.8216	.9013	.6362	.7576	.8395	.9124
		generated + real	.7938	.8784	.7898	.8753	.7717	.8620	.7916	.8752
WGAN-GP	Custom CNN	only generated	.4445	.5497	.7188	.8317	.6615	.7896	.6142	.7422
		generated + real	.7957	.8784	.7895	.8759	.7951	.8783	.7845	.8718

4.2 Augmented Classification

In Table 3, we can find classification scores after augmenting the training dataset with images generated by ACGANs. In Table 4 are the results of the other configurations. Each of these runs included 10,000 synthetic images, and half of them also used the real training set, bringing the total number of training samples to 29,557 images. We observe that classifiers with architectures more like the discriminator benefit from synthetic images. This could happen because the generated images encode the kind of information that architecture exploits best. This might explain, at least partially, why sometimes using only synthetic data helped more than the combination of real and synthetic images.

For ACGAN, SwinT is the discriminator that produced the most successful generator to improve classification performance, obtaining an F1-score of 90.43%. The overall best F1-score was obtained with data generated from the CGAN + ViT B 16 combination. Both of these high scores were obtained in the synthetic-only case, but the corresponding mixes with real data also improved the baseline.

4.3 Federated Learning

Here, we tried to replicate the performance of the centralized GAN experiments, this time in a federated environment. We can find classification scores with federated learning-augmented training data in Table 5. Because the number of clients affects the training time, the stability of the training, and overall performance, we analyzed two settings: one in

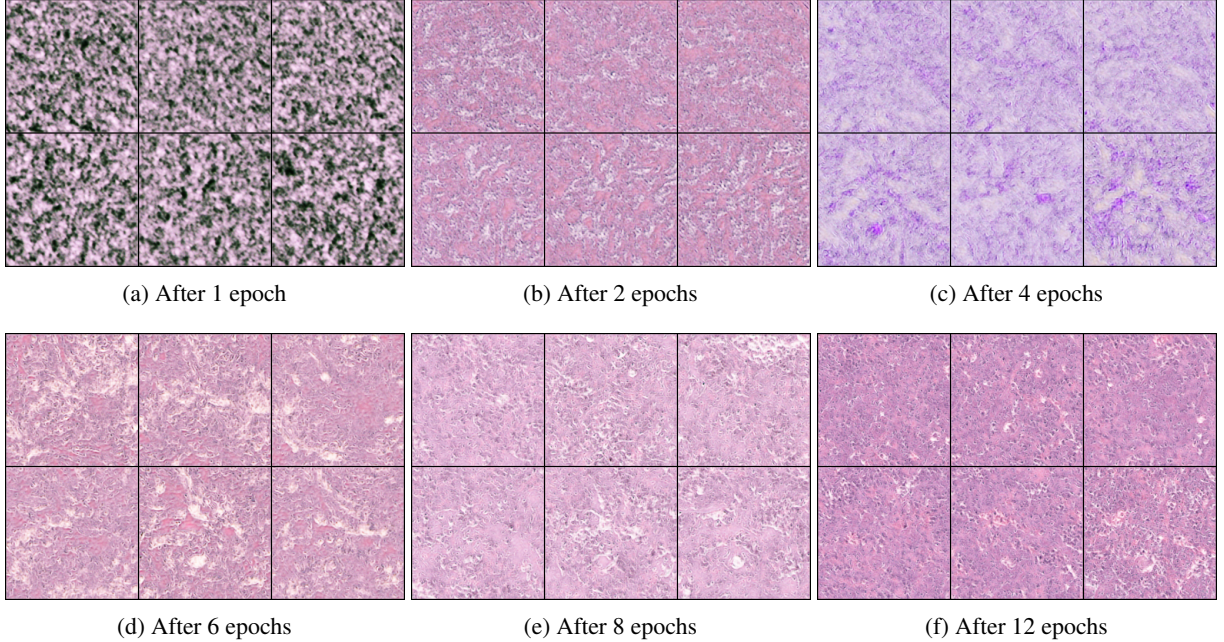


Figure 4: Examples of colonoscopy images when the non-IID ratio is 0.9. Note that an epoch here refers to a round of training the server model. Each round iterates over the client’s dataset multiple times.

Table 7: Classification scores when augmenting the training dataset with synthetic data from ACGAN + ViT, with different non-IID settings for FL clients. Improvements over the baseline (no synthetic data) are highlighted in bold.

Non-IID Ratio (%)	Data Type	ResNet 50		ViT B 16		ViT L 16		LeViT Conv 384	
		Acc.	F1	Acc.	F1	Acc.	F1	Acc.	F1
-	only real	.7965	.8800	.7952	.8802	.8005	.8833	.7846	.8713
60%	only generated	.8215	.9017	.7722	.8697	.7143	.8288	.8180	.8996
	generated + real	.7787	.8669	.7889	.8729	.7914	.8780	.7755	.8661
70%	only generated	.8370	.9112	.8381	.9117	.8363	.9105	.8364	.9108
	generated + real	.7805	.8699	.8023	.8850	.7822	.8691	.7797	.8686
80%	only generated	.2920	.3255	.3818	.4605	.2231	.1503	.1940	.0856
	generated + real	.8034	.8851	.7941	.8791	.7652	.8561	.7351	.8336
90%	only generated	.9358	.7450	.8019	.8896	.7837	.8753	.3839	.4596
	generated + real	.7895	.8758	.7931	.8763	.7917	.8772	.7923	.8774

4.3.2 Production-grade Setup

We implemented an experiment with a realistic setup to further test the feasibility of a federated learning system that spans multiple hospitals and allows them to keep their data private when training deep learning models. Using Kubernetes, we built a networked setup that used multiple actual nodes instead of simulating the network in software. Unlike an experimental setup, a more realistic one has to deal better with scalability, overhead issues, and security considerations.

Our implementation starts by creating a K8s cluster with a dedicated namespace that isolates our work from other tenants. We added GPU-enabled nodes to this cluster to support the high workload of running large machine learning models. For this experiment, we considered the case of four different hospitals (representing clients), and each of them was assigned to its node, which was used both to train the local version of the GAN and for communication with the server node. The aggregation server centralizes the model updates and coordinates training tasks throughout the network. A detailed diagram of this architecture can be seen in Figure 5.

The experiment was successful; we could use the entire cluster in parallel to train a version of the GAN with characteristics similar to those obtained in the federated setting described above.

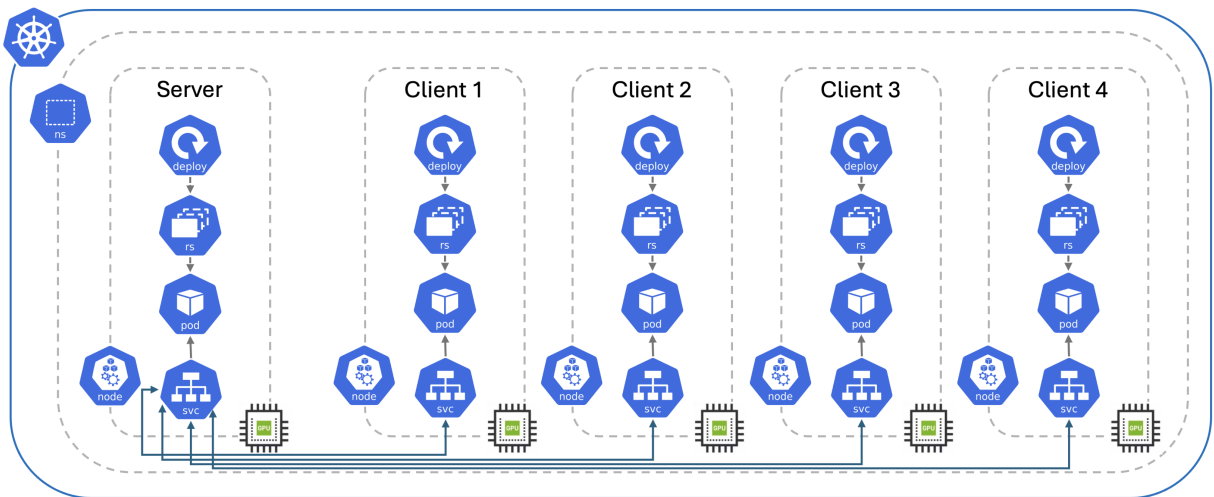


Figure 5: Kubernetes cluster architecture used for federated learning experiments.

5 Discussion

5.1 Did GANs Memorize the Training Data?

The memorization of training data is an issue that GANs are in danger of experiencing. The generator could learn to fool the discriminator by producing replicas of the training images. This would obtain a small loss value, but would not create a useful model since it would be unable to generate novel samples. However, our experiments did not show signs of this problem. Not only does the loss value not indicate this, but Figure 6 shows that the generated images are quite different from the ones in the training set.

5.2 Did mode collapse occur in GANs?

One common problem that GANs tend to experience is mode collapse, i.e., finding certain image types that manage to fool the discriminator and exploiting this by generating only images of those types. In our case, because the generator (i.e., CNN) and discriminator (i.e., ViT) fundamentally work differently, this helps to protect against mode collapse by introducing two different inductive biases. We can see that the model does not seem to experience mode collapse, generating many kinds for each image (for example, see Figures 3 and 6). However, we should note that the training set has much higher diversity, which is not reflected in the synthetic data.

5.3 Class Similarity

For our images to be useful for augmenting classification, we wish they encode some class-specific information. In addition to the classification scores presented before, we analyze them using data visualization. In Figure 7, we plot the embeddings produced by a ViT B 16 classifier for both real images and our synthetic images after reducing their dimension using the T-Distributed Stochastic Neighbor Embedding (t-SNE) technique [van der Maaten and Hinton, 2008]. We can see that, while the two plots have similar shapes, our synthetic samples have much less overlap in the central area. This could signify a lack of images that are harder to classify and could teach a model something new.

6 Conclusions

In this paper, we described the idea of augmenting classification datasets using synthetic data generated by GANs and experimented with it for a histological dataset. We compared multiple architectures and obtained promising results using ACGAN and ViT. We repeated experiments in the federated setting using Kubernetes as a production-ready framework. We concluded that this task and method are compatible with federated learning, which can have practical benefits in the medical context. Finally, we analyzed the images generated by ACGAN in more depth, searching for common problems that affect GANs, and observed that our method avoided some of these issues.

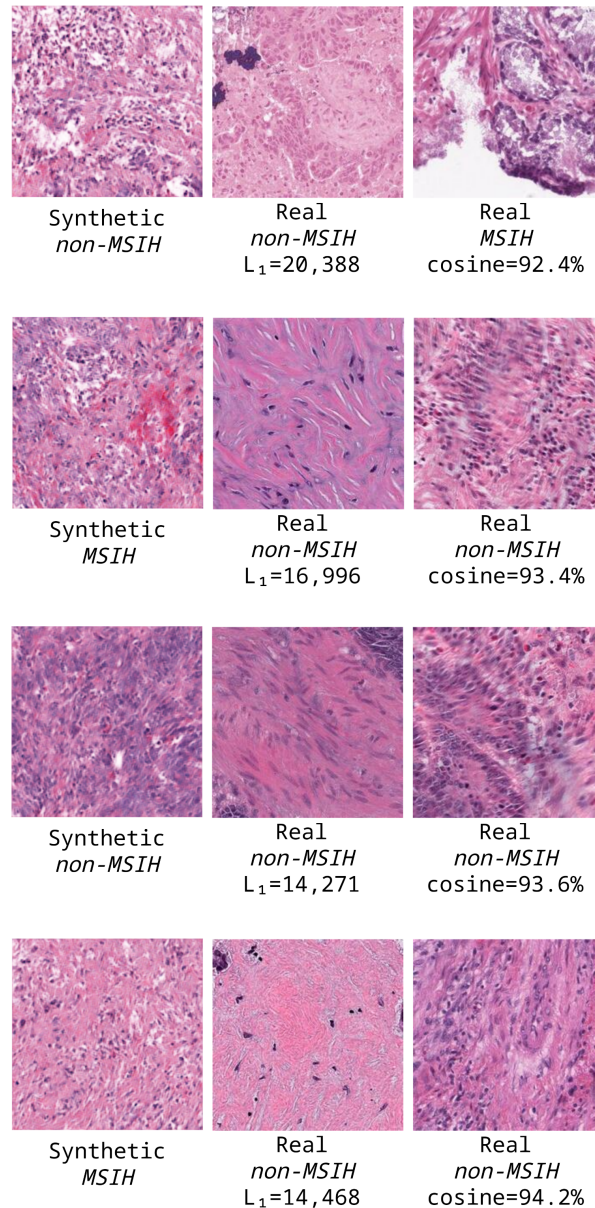


Figure 6: Comparison between four generated images and the training images closest to each. To measure similarity, we use the L_1 norm of the pixel-wise difference between the two images or the cosine similarity of the embeddings of the images. To compute embeddings, we use one of the classifiers trained on real images and treat one of its layers as a feature extractor.

Regarding future research, it could be helpful to investigate a similar method for a multi-class classification task (as opposed to the binary classification tackled here). Similarly, we could improve the final performance of this dataset by using more complex networks as components in the GAN or by stabilizing the training process. Finally, diffusion models [Ho et al., 2020] would constitute a different method of tackling the problem that has proven to be very effective and would merit comparison with the GAN approaches Huang et al. [2023].

Limitations

One limitation of our study is that, due to computational requirements, we did not perform extensive hyperparameter searches. The methods described here were susceptible to hyperparameters, so the results and conclusions could change

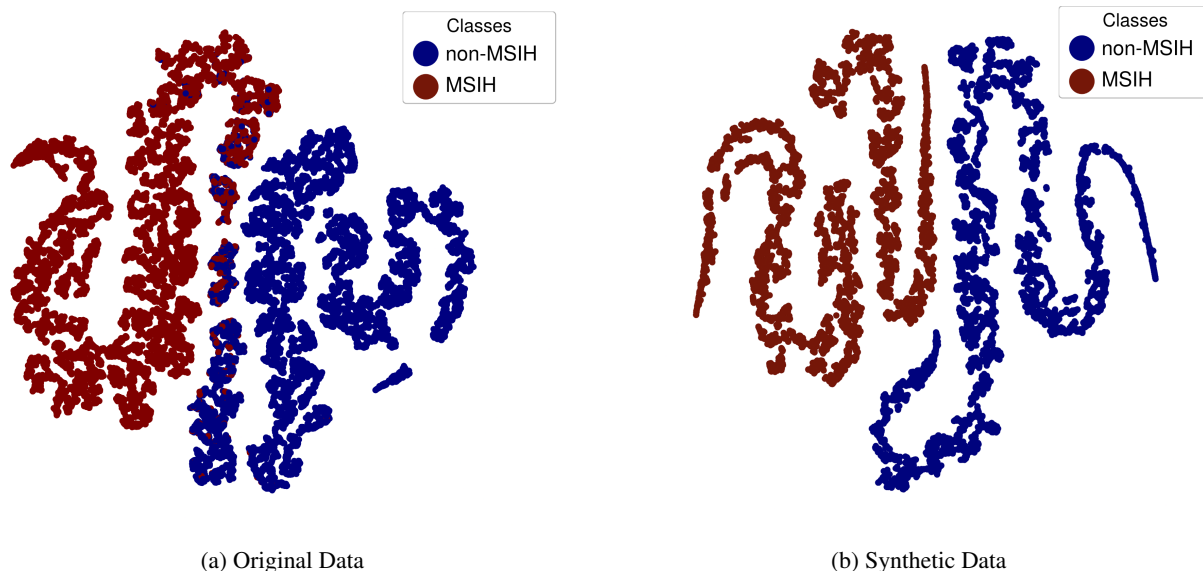


Figure 7: Visualization of original and synthetic data using t-SNE.

somewhat after a more thorough search. Another limitation is that we restricted the experiments to a single binary classification dataset. The lack of more diverse datasets might limit the conclusions we can draw from our results.

References

- M. Arjovsky, S. Chintala, and L. Bottou. Wasserstein generative adversarial networks. In D. Precup and Y. W. Teh, editors, *Proceedings of the 34th International Conference on Machine Learning*, volume 70 of *Proceedings of Machine Learning Research*, pages 214–223. PMLR, 06–11 Aug 2017. URL <https://proceedings.mlr.press/v70/arjovsky17a.html>.
- M. A. Bansal, D. R. Sharma, and D. M. Kathuria. A systematic review on data scarcity problem in deep learning: Solution and applications. *ACM Comput. Surv.*, 54(10s), sep 2022. ISSN 0360-0300. doi: 10.1145/3502287. URL <https://doi.org/10.1145/3502287>.
- D. J. Beutel, T. Topal, A. Mathur, X. Qiu, J. Fernandez-Marques, Y. Gao, L. Sani, K. H. Li, T. Parcollet, P. P. B. de Gusmão, and N. D. Lane. Flower: A friendly federated learning research framework, 2022.
- J. Deng, W. Dong, R. Socher, L.-J. Li, K. Li, and L. Fei-Fei. Imagenet: A large-scale hierarchical image database. In *2009 IEEE conference on computer vision and pattern recognition*, pages 248–255. Ieee, 2009.
- A. Dosovitskiy, L. Beyer, A. Kolesnikov, D. Weissenborn, X. Zhai, T. Unterthiner, M. Dehghani, M. Minderer, G. Heigold, S. Gelly, J. Uszkoreit, and N. Houlsby. An image is worth 16x16 words: Transformers for image recognition at scale. *CoRR*, abs/2010.11929, 2020. URL <https://arxiv.org/abs/2010.11929>.
- S.-V. Echim, R.-A. Smădu, A.-M. Avram, D.-C. Cercel, and F. Pop. Adversarial capsule networks for romanian satire detection and sentiment analysis. In *International Conference on Applications of Natural Language to Information Systems*, pages 428–442. Springer, 2023.
- P. Esser, R. Rombach, and B. Ommer. Taming transformers for high-resolution image synthesis. In *Proceedings of the IEEE/CVF conference on computer vision and pattern recognition*, pages 12873–12883, 2021.
- W. Falcon and The PyTorch Lightning team. Pytorch lightning, mar 2019. URL <https://github.com/Lightning-AI/lightning>.
- M. L. Fang, D. S. Dhama, and K. Kersting. Dp-ctgan: Differentially private medical data generation using ctgans. In *International Conference on Artificial Intelligence in Medicine*, pages 178–188. Springer, 2022.
- I. Feki, S. Ammar, Y. Kessentini, and K. Muhammad. Federated learning for covid-19 screening from chest x-ray images. *Applied Soft Computing*, 106:107330, 2021.
- I. Goodfellow, J. Pouget-Abadie, M. Mirza, B. Xu, D. Warde-Farley, S. Ozair, A. Courville, and Y. Bengio. Generative adversarial nets. *Advances in neural information processing systems*, 27, 2014.

- B. Graham, A. El-Nouby, H. Touvron, P. Stock, A. Joulin, H. J'egou, and M. Douze. Levit: a vision transformer in convnet's clothing for faster inference. *2021 IEEE/CVF International Conference on Computer Vision (ICCV)*, pages 12239–12249, 2021. URL <https://api.semanticscholar.org/CorpusID:233004577>.
- I. Gulrajani, F. Ahmed, M. Arjovsky, V. Dumoulin, and A. Courville. Improved training of wasserstein gans. In *Proceedings of the 31st International Conference on Neural Information Processing Systems, NIPS'17*, page 5769–5779, Red Hook, NY, USA, 2017. Curran Associates Inc. ISBN 9781510860964.
- K. He, X. Zhang, S. Ren, and J. Sun. Deep residual learning for image recognition. In *Proceedings of the IEEE conference on computer vision and pattern recognition*, pages 770–778, 2016.
- M. Heusel, H. Ramsauer, T. Unterthiner, B. Nessler, G. Klambauer, and S. Hochreiter. Gans trained by a two time-scale update rule converge to a nash equilibrium. *CoRR*, abs/1706.08500, 2017. URL <http://arxiv.org/abs/1706.08500>.
- J. Ho, A. Jain, and P. Abbeel. Denoising diffusion probabilistic models. *Advances in neural information processing systems*, 33:6840–6851, 2020.
- R. Huang, Y. Ren, Z. Jiang, C. Cui, J. Liu, and Z. Zhao. Fastdiff 2: Revisiting and incorporating gans and diffusion models in high-fidelity speech synthesis. In *Findings of the Association for Computational Linguistics: ACL 2023*, pages 6994–7009, 2023.
- L. Jose, S. Liu, C. Russo, A. Nadort, and A. Di Ieva. Generative adversarial networks in digital pathology and histopathological image processing: A review. *Journal of Pathology Informatics*, 12(1):43, 2021. ISSN 2153-3539. doi: https://doi.org/10.4103/jpi.jpi_103_20. URL <https://www.sciencedirect.com/science/article/pii/S2153353922001651>.
- J. N. Kather. Histological image tiles for tcga-crc-dx, color- normalized, sorted by msi status, train/test split, may 2020. URL <https://doi.org/10.5281/zenodo.3832231>.
- Z. Liu, Y. Lin, Y. Cao, H. Hu, Y. Wei, Z. Zhang, S. Lin, and B. Guo. Swin transformer: Hierarchical vision transformer using shifted windows. *2021 IEEE/CVF International Conference on Computer Vision (ICCV)*, pages 9992–10002, 2021. URL <https://api.semanticscholar.org/CorpusID:232352874>.
- T. maintainers and contributors. Torchvision: Pytorch's computer vision library. <https://github.com/pytorch/vision>, 2016.
- O. N. Manzari, H. Ahmadabadi, H. Kashiani, S. B. Shokouhi, and A. Ayatollahi. Medvit: a robust vision transformer for generalized medical image classification. *Computers in Biology and Medicine*, 157:106791, 2023.
- B. McMahan, E. Moore, D. Ramage, S. Hampson, and B. A. y Arcas. Communication-efficient learning of deep networks from decentralized data. In *Artificial intelligence and statistics*, pages 1273–1282. PMLR, 2017.
- A. Mino and G. Spanakis. Logan: Generating logos with a generative adversarial neural network conditioned on color. In *2018 17th IEEE International Conference on Machine Learning and Applications (ICMLA)*, pages 965–970. IEEE, 2018.
- M. Mirza and S. Osindero. Conditional generative adversarial nets. *arXiv preprint arXiv:1411.1784*, 2014.
- G.-S. Năstăsescu and D.-C. Cercel. Conditional wasserstein gan for energy load forecasting in large buildings. In *2022 International Joint Conference on Neural Networks (IJCNN)*, pages 1–8. IEEE, 2022.
- Nicki Skafte Detlefsen, Jiri Borovec, Justus Schock, Ananya Harsh, Teddy Koker, Luca Di Liello, Daniel Stancil, Changsheng Quan, Maxim Grechkin, and William Falcon. Torchmetrics - measuring reproducibility in pytorch, feb 2022. URL <https://github.com/Lightning-AI/torchmetrics>.
- A. Odena, C. Olah, and J. Shlens. Conditional image synthesis with auxiliary classifier gans. In *International conference on machine learning*, pages 2642–2651. PMLR, 2017.
- K. O'shea and R. Nash. An introduction to convolutional neural networks. *arXiv preprint arXiv:1511.08458*, 2015.
- A. Paraschiv and D.-C. Cercel. Upb at germeval-2019 task 2: Bert-based offensive language classification of german tweets. In *KONVENS*, 2019.
- A. Paraschiv, D.-C. Cercel, and M. Dascalu. Upb at semeval-2020 task 11: Propaganda detection with domain-specific trained bert. In *Proceedings of the Fourteenth Workshop on Semantic Evaluation*, pages 1853–1857, 2020.
- A. Paszke, S. Gross, F. Massa, A. Lerer, J. Bradbury, G. Chanan, T. Killeen, Z. Lin, N. Gimeshein, L. Antiga, et al. Pytorch: An imperative style, high-performance deep learning library. *Advances in neural information processing systems*, 32, 2019.

- B. Pfitzner, N. Steckhan, and B. Arnrich. Federated learning in a medical context: A systematic literature review. *ACM Trans. Internet Technol.*, 21(2), jun 2021. ISSN 1533-5399. doi: 10.1145/3412357. URL <https://doi.org/10.1145/3412357>.
- M.-A. Tanase, D.-C. Cercel, and C. Chiru. Upb at semeval-2020 task 12: Multilingual offensive language detection on social media by fine-tuning a variety of bert-based models. In *Proceedings of the Fourteenth Workshop on Semantic Evaluation*, pages 2222–2231, 2020.
- L. van der Maaten and G. Hinton. Visualizing data using t-sne. *Journal of Machine Learning Research*, 9(86): 2579–2605, 2008. URL <http://jmlr.org/papers/v9/vandermaaten08a.html>.
- A. Vaswani, N. Shazeer, N. Parmar, J. Uszkoreit, L. Jones, A. N. Gomez, Ł. Kaiser, and I. Polosukhin. Attention is all you need. *Advances in neural information processing systems*, 30, 2017.
- G.-A. Vlad, M.-A. Tanase, C. Onose, and D.-C. Cercel. Sentence-level propaganda detection in news articles with transfer learning and bert-bilstm-capsule model. In *Proceedings of the Second Workshop on Natural Language Processing for Internet Freedom: Censorship, Disinformation, and Propaganda*, pages 148–154, 2019.
- G.-A. Vlad, G.-E. Zaharia, D.-C. Cercel, C. Chiru, and S. Trausan-Matu. Upb at semeval-2020 task 8: Joint textual and visual modeling in a multi-task learning architecture for memotion analysis. In *Proceedings of the Fourteenth Workshop on Semantic Evaluation*, pages 1208–1214, 2020a.
- G.-A. Vlad, G.-E. Zaharia, D.-C. Cercel, and M. Dascalu. Upb@ dankmemes: Italian memes analysis-employing visual models and graph convolutional networks for meme identification and hate speech detection. In *Proceedings of Seventh Evaluation Campaign of Natural Language Processing and Speech Tools for Italian. Final Workshop (EVALITA 2020)*, Online. CEUR.org, 2020b.
- R. Wightman. Pytorch image models. <https://github.com/rwightman/pytorch-image-models>, 2019.
- X. Xu, S. Kapse, R. Gupta, and P. Prasanna. Vit-dae: Transformer-driven diffusion autoencoder for histopathology image analysis. In A. Mukhopadhyay, I. Oksuz, S. Engelhardt, D. Zhu, and Y. Yuan, editors, *Deep Generative Models*, pages 66–76, Cham, 2024. Springer Nature Switzerland. ISBN 978-3-031-53767-7.
- L. Zedda, A. Loddo, and C. Di Ruberto. Hierarchical pretrained backbone vision transformer for image classification in histopathology. In *International Conference on Image Analysis and Processing*, pages 223–234. Springer, 2023.